The Erosive Axial Collapse of a Cavitating Vortex: An Experimental Study

M. A. Dominguez-Cortazar, Jean-Pierre Franc, Jean-Marie Michel

The Erosive Axial Collapse of a Cavitating Vortex: An Experimental Study

M. A. Dominguez-Cortazar
Assistant,
Centro University,
Queretaro, Mexico

J. P. Franc
Research Assistant.

J. M. Michel
Research Director.

Laboratoire des Écoulements
Géophysiques et Industriels,
Institut de Mécanique de Grenoble,
BP 53, 38041 Grenoble Cédex 9, France

The erosive efficiency of cavitating vortices is well known, although its exact mechanism has not been clarified. In order to bring fundamental information to the subject, a new device called ''Cavermod'' was designed in which axial collapse of a cavitating vortex is produced. We consider in this paper the design principles of the apparatus, the measurement equipment necessary for observing the phenomenon (collapse time of the order of a few milliseconds, axial collapse velocity varying between 70 and 700 m/s), and the main features of the flow. We also study the damage produced on erosion targets in order to correlate the vortex collapse with the erosion indentation features.

1 Introduction

The study of fundamental hydrodynamic mechanisms in cavitation erosion has been the subject of many research works and publications for about thirty years. In general, the research effort was directed to the situation in which a bubble collapses and rebounds, either producing high pressures and shock waves in its vicinity or giving a small re-entrant jet in the case of symmetry defect. It has been both theoretically and experimentally shown that if a cavitation bubble collapses near a rigid wall, it produces a very high-pressure over a small area of the solid surface. It has also been found that the impulsive pressure is strongly dependent on the distance of the bubble to the solid wall. Well-known papers are associated with those models, among them the studies of Hickling and Plesset (1963), Benjamin and Ellis (1966), Plesset and Chapman (1971), Lauterborn and Bolle (1975), Fujikawa and Akamatsu (1980), Blake et al. (1987), and Tomita and Shima (1986).

As well as bubble collapse, damage is also associated with the collapse of cavitating vortices. Selim and Hutton (1983) show that the wakes of partial cavities, in which a number of cavitating vortices are shed, seem to be intense sources of erosion. Soyama et al. (1992) also report that the cavitation erosion in hydraulic machinery is particularly severe when cavitation vortices are shed from the rear part of an attached cavity and collapse rapidly in the vicinity of a solid wall. This was at the origin of the development of the so-called Cavitation Vortex Generator devised by Lecoffre (1978) and realized by Lecoffre et al. (1981). In this device, a cavitating vortex is created then annihilated by successively closing and opening a valve on the input flow line of a conical chamber. It appears to be an efficient tool for carrying out metallurgical tests, see e.g., Karimi (1988). Very high speed visualizations of the vortex collapse by Avellan and Farhat (1989) have shown that it is mainly axial for most of its duration. However, the final stage is marked by the emission of spherical shock waves from several points which resemble collapsing bubbles. Thus, the situation is not simple and requires further examination.

In order to provide fundamental information about this subject, a special device called ''Cavermod'' (abbreviation of CAVitation ERosion MODel) was designed. Like the Vortex Generator, this device uses the axial collapse of a cavitating vortex, but here the vortex is created in a closed rotating chamber, filled with deaerated liquid. The volume of the chamber can be slightly increased in order to form a vapor core in the vicinity of the rotation axis; then it is suddenly decreased in such a way that an axial collapse of the vapour core is produced. Of course the basic motion of the liquid is a solid rotation and not a true vortex; it must be noted that a solid rotation is also found in the central region of the Vortex Generator.

In industrial situations, cavitating vortices appear either as continuous vapor cores or as chains of bubbles entrapped in the low pressure vorticity filaments. Their axial collapse can occur if they are properly directed relative to the ambient pressure gradient and/or the local directions of the strain rate tensor (example of such situations in case of a wake shear flow can be found in Belahadji et al., 1995). When these favorable conditions are fulfilled, a continuous core should disappear approximately as shown in the present paper whereas bubble chains would probably result in cascade mechanisms. In the present study, only the axial collapse of a vortex is studied, but the formation and collapse of a spinning bubble chain is possible and its study remains an interesting objective.

2 Basic Ideas

The first point to be examined concerns the transfer of mechanical energy from the liquid flow to the solid wall, by which erosion is brought about. Such a transfer needs two conditions be satisfied: a high level of stress, in order to exceed some limit of material resistance, for example the yield stress, and a loading time sufficient to make nonreversible transformation of the solid material. Concerning this last point, the shock wave coming from the bubble collapse and rebound, as calculated for example by Fujikawa and Akamatsu (1980), seems to give times of an order lower than one microsecond. If we consider microjets of diameter d, the time of the impulse they transmit to the wall is of the order $d/2C$, where C is the sound velocity in water. With current values of d (lower than 1 mm), we obtain 0.3 μs. It will be shown below that, due mainly to the larger size of the impact area, greater loading times are obtained with the present apparatus.

The second point is related to the physical model used in the design of the apparatus (Fig. 1). The solid rotation of a body of liquid with a central vapour core is created in a rotating chamber closed on one side by a piston. The piston plays the role of a wave-maker for that free surface flow in which gravity is replaced by the centrifugal forces. The required axial collapse can be obtained if the piston moves rapidly enough toward the chamber interior, creating a steeply fronted wave which progressively fills the vortex core. With a rigid cylindrical

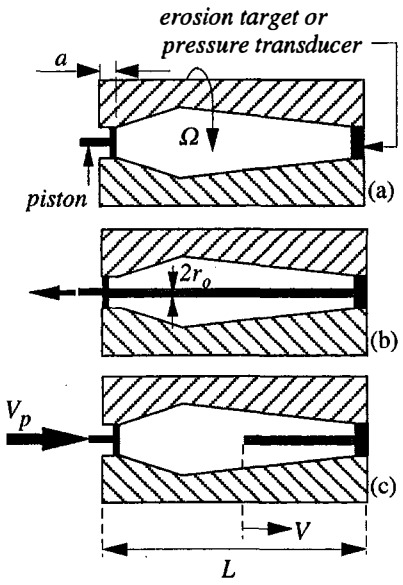

Fig. 1 Principle of the apparatus

chamber (radius R), calculations based on conservation of mass and momentum of an incompressible fluid are rather simple (Dominguez-Cortazar 1994). The main results are the following: (a) The minimum value of the piston speed required to obtain a wave to fill the vapor core is:

$$V_p \geq [redacted]$$

In current circumstances, that limiting value is quite small and it can be easily obtained. For example we obtain about 0.2 m/s with R = 20 mm, r_0 = 3.3 mm, Ω = 4000 rpm (b) Then the axial collapse velocity V is related to V_p by the following relation:

$$V = V_p \frac{L}{a} = V_p \frac{R^2}{r_o^2}$$

Very large collapse velocities can be thus obtained. In the case when r_o becomes very small (which indeed needs a higher rotation speed, as mentioned in Section 3), these relations would give infinite values for V. In fact, two main mechanisms tend to limit the V-values: on one hand the compressibility effects and on the other, the volume expansion of the rotating chamber under centrifugal forces. These effects are not taken in acount in the last relations.

A rough estimate of the loading characteristics can be made if we suppose that the wave has a front perpendicular to the axis of the chamber. If that was the case, the value of the overpressure produced at the end of the collapse on the target or the pressure transducer would be expressed approximately by the water hammer formula:

$$P = \rho C V$$

which gives about 1500 bars with V = 100 m/s. The loading time can be estimated from the expression r_o/C, which gives 2.3 μs for r_o = 3.3 mm. It must be understood that this model gives rather extreme values: actually, the core vortex closure does not take the shape of a wave with a steep front, but rather it resembles an ogive with length l of 10 mm (see Fig. 4 for example). Then the end of the collapse takes a larger time of the order of l/V, ie about 0.1 or 0.01 ms, while the overpressure is smaller than the one given by the water hammer formula. Despite these differences, Cavermod proves to be very efficient in producing cavitation erosion.

3 The Experimental Apparatus

The main part of Cavermod is a closed rotating chamber filled with water. It is made of plexiglas in order to allow observation of the phenomena. At one end of the chamber, a pressure transducer or an erosion target is mounted to receive the collapse impact. At the other end, the chamber is closed by a piston and a rubber membrane. To make its complete filling with deaerated water easier, the internal geometry of the chamber is biconical.

The operating principle is shown in Fig. 1. The chamber filled with dearated water rotates at velocity Ω (Fig. 1(a)); the control system allows the axial displacement of the piston, a, which results in the volume increase of the chamber and in the appearance of the vapor core (Fig. 1(b)). Then, a sudden volume reduction, due to the shock of a projectile against the piston head, produces the expected cavity collapse (Fig. 1(c)). In addition to the control of the three main parameters of the flow, Ω, r_o and V, some other less important advantages can also be expected from this configuration, for instance the concentration of the erosive impacts on a small area of the solid wall (some square millimeters) around the rotation axis and the use of liquids other than water.

The initial size of the vapor core is given by the conservation of the liquid volume. For a given size of the cavity, the axial collapse velocity is controlled by the driving pressure of the projectile Δp (which controls the shock intensity between the projectile and the piston head). That driving pressure is ensured by a pneumatic system: thus, by adjusting a and Δp, we can control two fundamental parameters of the flow: r_o and V. This means that all kinds of vortex collapses (from the weakest to the most violent) can be realised. However, the minimum radius of the cavity is limited by the maximum rotation velocity of the chamber via the stability condition given by Rosenthal (1962): the vapor core radius has to be larger than a critical value expressed as

$$r_{oc} = (4S/\rho\Omega^2)^{1/3}$$

where S is the surface tension. This equation gives 1.18 mm for the maximum rotation rate of 4000 rpm in the case of water. The sketch of the apparatus is shown in Fig. 2. The main design values are:

—Length of the test chamber	(L)	156 mm
—Piston displacement range	(a)	1 to 4 mm
—Chamber rotation range	(Ω)	0 to 4000 rpm
—Piston displacement velocity	(V_p)	0 to 6 m/s
—Driving pressure of the projectile	(Δp)	0 to 6 bars.

Nomenclature

a = piston displacement (mm)
C = sound velocity in water (m/s)
L = chamber length (mm)
r_o = initial radius of the vortex (mm)
R = piston radius (mm)
V = axial collapse velocity of the vortex (m/s)
V_p = piston displacement velocity (m/s)
P = impact pressure against the solid wall (Mpa)
Δp = driving pressure of the projectile (bars)
ρ = water density (kg/m3)
Ω = chamber rotation rate (rd/s)

Return now to the fundamental parameters of the flow. From the radius R of the equivalent cylindrical chamber, the length L, the radius r_o, the collapse velocity V, and the rotation rate Ω, it is possible to build three dimensionless numbers, the most important of them being the Rossby number $\Omega r_o/V$. As this number is very small in the normal running conditions, it might be inferred that Coriolis forces do not play an important role at first sight. Then, in order to model the flow numerically, it becomes possible to assume that in the rotating frame the flow is irrotational, which permits to use simplified techniques issued from the boundary integral method (Dominguez-Cortazar and Canot, 1995). Such methods result in the formation of a reentrant jet in the closure region of the vortex core. However, experimental tests do not show such a jet (see Section 5). Consequently, in spite of the small value of the Rossby number, it seems that Coriolis forces, by which the total axial moment of momentum of the liquid body remains constant during the vortex collapse, have to be taken in account for a correct representation of the Cavermod flow.

In addition to the previous discussion, dynamical parameters such as the liquid density ρ and the vapor pressure p_v should first be outlined. However, consideration of a cavitation parameter is not pertinent: on the one hand, no ambient pressure can be defined in the chamber before the formation of the vapor core, and on the other, when the vapor core appears, the pressure in the chamber is fixed by the vapor pressure near the axis. Then, as far as delays due to vaporization processes can be neglected and global flow behavior only is considered, comparison with real situations has to be made mainly on the basis of the Rossby number. If one is interested also in the final stage of the collapse and the splitting up phenomena (there is experimental evidence that the end of the first collapse is marked by a large number of local erosive events, the size of which is lower than the radius r_o by one order of magnitude at least), one must also take into account the liquid surface tension and the Weber similarity. Of course, the overpressure produced on the erosion targets will be mainly correlated by the collapse velocity V, the speed of sound C and the liquid density ρ, while the loading duration should be referred either to the time r_o/C or to the time l/V, where l is the length of the ogive in the collapsing zone, as previously discussed.

4 Specific Instrumentation and Uncertainties

The flow produced in the Cavermod is highly unsteady and the cavitation vortices are characterized by a total lifetime of about few milliseconds. In consequence various visualization techniques are needed for experimental study. The first one, a high speed camera, PHOTEC (up to 40,000 frames per second), has been used to record the main events of the phenomenon. However, the maximum rotation speed of its driving motor is not high enough (with a minimum interframe of 25 μs) so, only a few images of the first vortex collapse can be obtained. For the second visualization device, one takes advantage of the fact that the flow is fairly repeatable from one shot to the other when all control parameters are kept the same. The photographs can be taken under flash lighting which is triggered at increasing times from an initial instant given by a shock accelerometer.

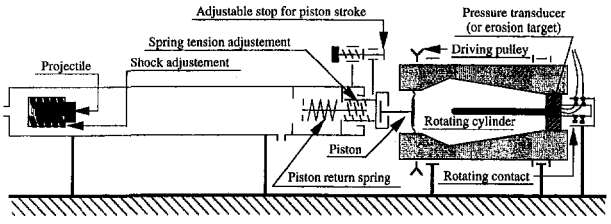

Fig. 2 The main mechanical elements of Cavermod

The light source is a Palflash 500 (from HADLAND Corp.) with light-pulse of about 250 ns. In this way it is possible to reconstitute the sequence of the first vortex collapse. The same device was used to measure the piston displacement as a function of time.

The vortex collapse velocity, just before its terminal phase, is measured by means of two parallel laser beams separated by 40 mm, which are received by two photoelectric cells in the absence of vortex and are occulted by the interface of the hollow vortex. Both signals are transfered to a digital oscilloscope, NICOLLET, with high acquisition rate (200 MHz), which enables measurements of the time interval between the two laser beams.

A piezo-electric pressure transducer (PCB 109A, diameter 6.3 mm, resonant frequency 500 kHz and rise time of about 1 μs) is flush-mounted at the end section of the chamber opposite to the piston (Fig. 1). Its signal is proportional to the total force it sustains, subject to the condition that its rise time is small enough (Vogel and Lauterborn, 1989). Even though its size is significantly larger than the size of the erosive events, we can at least deduce the mean pressure on the target as a function of time (Le et al., 1993).

The error on geometrical parameters (chamber length L, piston radius R) can be considered as negligible. For the fundamental quantities, the uncertainties are the following: 1 percent for Ω, 0.05 mm for a, 0.1 bar for Δp. Despite of the geometrical relation between r_o, R, L, and a, the r_o-error is quite large due to the additional effect of centrifugal forces on the chamber volume (see Section 2): it can be estimated as 0.3 mm. The uncertainty on the collapse velocity is about 10 percent. In Fig. 6, the error on abscissae (time) is considered negligible, while the ordinates (tension) cannot be related precisely to a pressure value. The error on the vortex length is 3 mm. Finally in Fig. 8, the size of indentations is known within a range of about 5 percent. All those values are estimated as maximum values.

5 Main Features of the Flow

Figure 3 shows a schematic résumé of the main events recorded with the high speed camera. In general, four rebounds are observed, but only two are represented. Some interesting features of the flow can be observed on this diagram. First, the linear variation of the vortex length proves that the first collapse is mainly axial and the measured velocity V is really typical of all the first collapse. Second, for the present experimental conditions, the duration of the axial stage of the collapse is about 0.3 ms. After the first collapse, subsequent formation and disappearance of the cavity are of radial type because the velocity of the secondary piston displacement becomes smaller than the critical value needed by the axial collapse.

Figure 4 shows a sequence of photographs of the first implosion reconstructed from separated shots. It confirms the axial nature of the vortex collapse. During the first instants, the free surface of the cavity appears to be unperturbed outside of the closure region. This one appears whitish and its details are not clear. Nevertheless, one can see some spots of interface instabilities on several images. The left end of the whitish region moves with a speed two or three times larger than the vortex closure and quickly invades all the cavity length.

The propagation of the whitish region produces, in the neighborhood of the target side, a kind of two-phase torus whose internal diameter is approximately equal to the initial diameter of the vapour core.

From the first instants of the collapse, on the right side of the closure region, we observe a narrow vapour core near the piston together with a more or less helicoidal vapour residue which follows the closure region of the cavity. The vapor residue is in good agreement with the conservation of local moment of momentum, which prevents the liquid elements from reaching the axis of rotation.

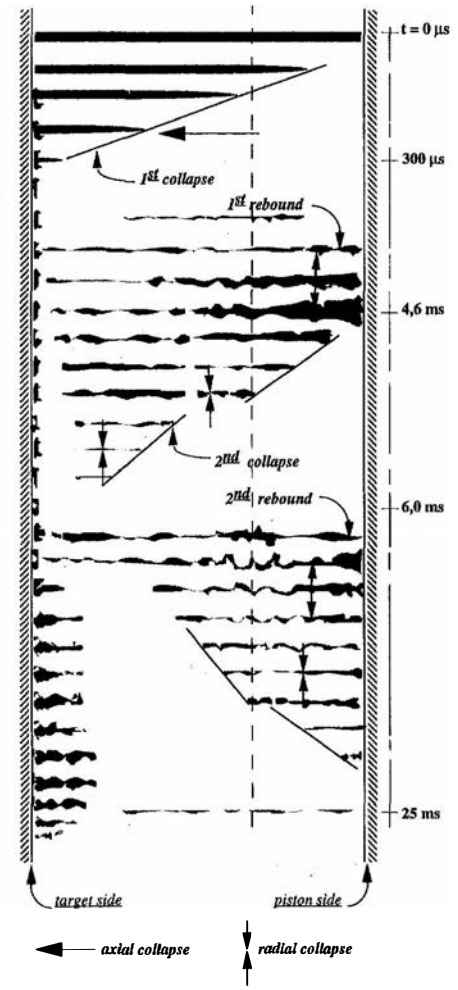

Fig. 3 Schematic diagram of the main events during the total collapse time (Δp = 3 bars, r_o = 1.6 mm, Ω = 3500 rpm)

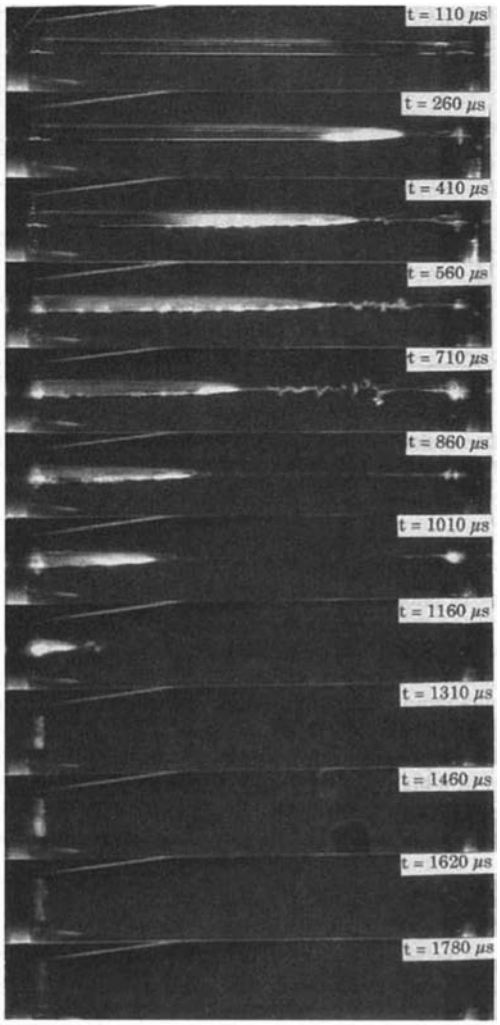

Fig. 4 *The first collapse of the cavity* (Ω = 3500 rpm, r_o = 2.9 mm, Δp = 1.0 bar)

The axial collapse velocity measured with the laser beam system is shown in Fig. 5 for several experimental conditions. These values are of the same order of magnitude as the velocity values estimated with the high speed camera. For a given value of the shock pressure Δp, the axial collapse velocity is as large as the initial size of the cavity is small. In the case of the smaller Δp-values, the dependence of the collapse velocity on the inverse of the vapor core area is almost linear, so that it can be inferred that the geometric effect is prominent. In the case of larger Δp-values, the results are less clear. In particular, the maximum collapse velocity seems to be not very dependent on the driving pressure (attention must be paid to the large uncertainties in Fig. 5). On the whole, for a first approach and if we assume that the high pressure during the vortex collapse is due to the rapid axial velocity of the interface which strikes the solid wall, the smaller cavities must be more aggressive than the larger one. For instance (at the same Δp value of 1 bar), in the case of a cavity of r_o = 2.9 mm, the axial velocity V is about 100 m/s and the order of magnitude of the impact pressure, estimated from the water hammer formula $P = \rho CV$, is around 140 Mpa whereas it is equal to 540 Mpa if r_o = 1.6 mm, because V = 390 m/s. As already mentioned, that assertion has to be tempered by consideration of the loading time (which decreases with the vapor core radius) and also of the limiting effects of compressibility.

The direct pressure measurements give, at the final stage of the first collapse, about eight pressure peaks. The results obtained from the transducer were only qualitative because the amplitude signal is strongly dependent on the transducer area and on the frequency ratio between the transducer characteristics and those of the final stage collapse (Dominguez, 1994). However, the transducer allowed us a temporal characterisation of the main events of the phenomenon.

The pressure peaks seem to have the same duration as other classical cavitating structures (some microseconds). Figure 6 shows a temporal correlation between the evolution of the vortex length and the instant when the impulsive pressure appears.

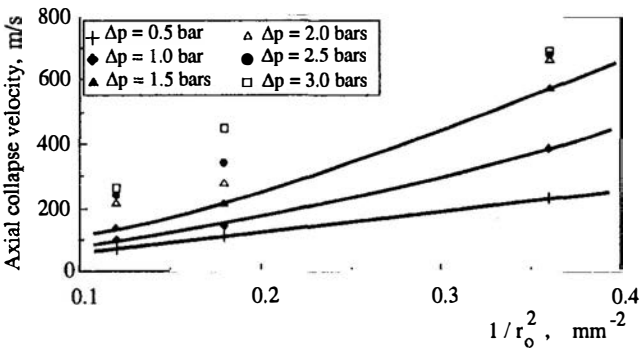

Fig. 5 Variation of the axial velocity versus the initial size of the vapour core (Ω = 3500 rpm, relative uncertainties: $\delta\Delta p$ = 0.1 bar, $\delta V/V$ = 10%, $\delta(1/r_o^2)/1/r_o^2$ = 20%)

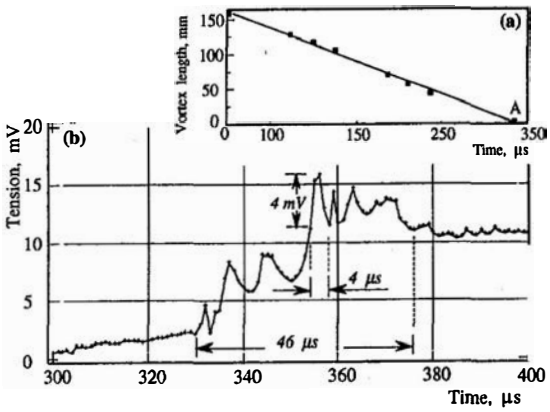

Fig. 6 Correlation between the axial vortex collapse and the impulsive pressure peaks (Ω = 3500 rpm, r_o = 1.6 mm, Δp = 1.0 bar, δl = 3 mm)

At time t = 330 μs (cf. point A, Fig. 6(a)), which corresponds to the final minimum length of the vortex (as deduced from a sequence of photographs of Fig. 4), we observe the first impulsive peak on the pressure signal (cf. Fig. 6(b)).

Thus the first pressure peak in Fig. 6 is attributed to the impact from the interface vapour-liquid, when the ogive apex of the closure region reaches the pressure transducer. This interface impact probably results in the creation of tiny new bubbles due to the disintegration of the two-phase torus. These bubbles are exposed to a high-pressure field so that they may collapse rapidly. Consequently we note, in a very short time interval of about 50 μs, multiple pressure peaks like those shown in Fig. 6.

6 Erosion Tests

Erosion tests on various materials (stainless steel, bronze, copper, brass, and aluminium targets) are carried out with deareated distilled water (water is considered fully deaerated if no air bubbles appear after a shot). The erosive efficiency of the Cavermod has been successfully demonstrated. Indeed, with a single shot we obtain multiple erosion pits. After every shot, the pits have been observed with a differential interference microscope (Nikon Optiphot). The erosion damage at the surface of the test piece is analysed by the number, size and depth of the pits. The influence of the axial collapse velocity, initial size of the vortex and shot number on damage have been studied. We also studied the spatial distribution of the pits in order to correlate the vortex collapse and the erosion indentations features.

Figure 7 shows the damage patterns caused on pure aluminium targets (Vickers Hardness 50) and under increasing Δp values. Each test corresponds to a single shot. As the driving pressure of the piston increases, the damage pattern increases. However, the average diameter of the damage pattern is conserved because the three tests are carried out with the same initial size of the vapour core. In some cases, as with Δp = 6 bars (cf. Fig. 7(c)), the density of erosion pits is so high that they cannot be counted: in such a limiting case, the erosion pattern can be considered as due to the implosion of the vortex itself.

The numerous indentations illustrate the complexity of the final stage of collapse. However, by studying the damage pattern, some interesting observations can be drawn:

- Every vortex collapse is characterized by a nearly circular erosion spot. The size of this spot is approximately equal to the initial core diameter. It is formed by numerous indentations of very different sizes. In general, large indentations appear on the erosion spot periphery and the smaller in the central part.

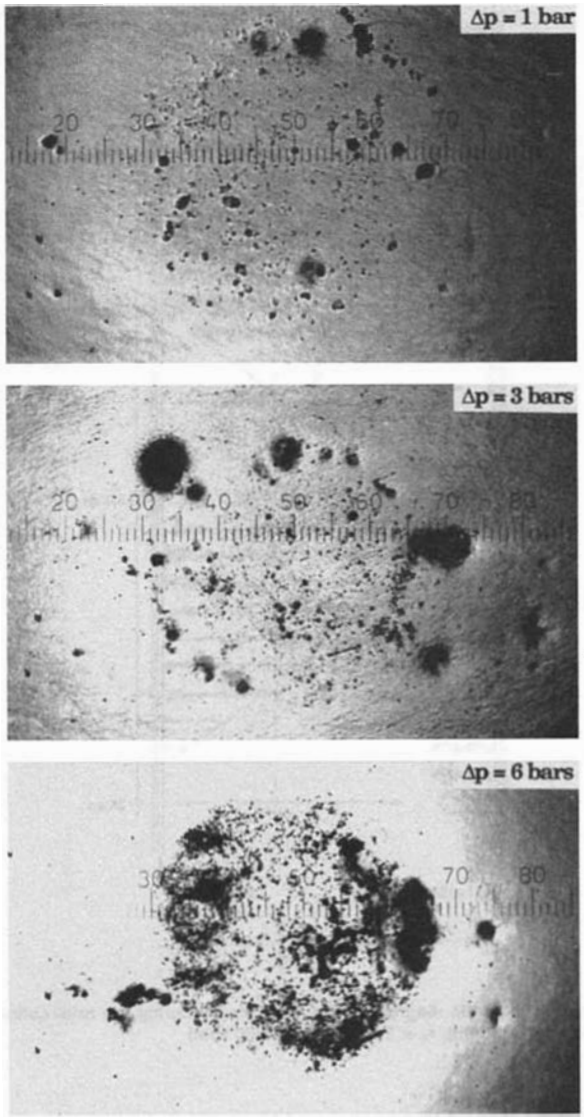

Fig. 7 Erosion patterns on aluminium Ω = 3500 rpm, r_o = 1.6 mm (10 div. = 0.62 mm)

- After a single shot, the indentation distribution is often asymmetric: this means that the indentations appear on about $\frac{2}{3}$ of the total polar section. This observation seems to be related to photographic visualisation, which shows that the perturbations on the free surface of the vortex are not symmetrical with respect to the rotation axis.
- As regards the size of indentations (from some μm to 500 μm), the maximum number occurs for the sizes smaller than 10 μm in radius (cf. Fig. 8, for several experi-

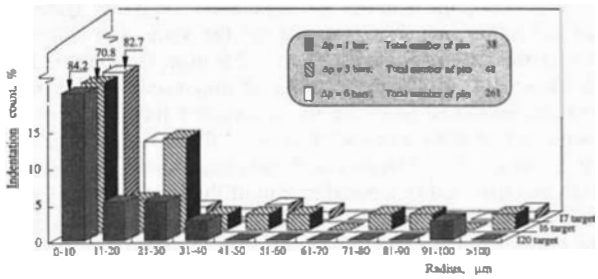

Fig. 8 Distribution of indentation sizes on stainless steel specimens (Ω = 3500 rpm, r_o = 1.6 mm, uncertainty of 5% on the indentation radii)

mental conditions, with stainless steel 316 L, Vickers hardness 150). Nevertheless, the main contribution to the total volume eroded is provided by the largest indentations.

- For long-term exposure, shots produce indentations at a proportional rate. The number, the size, and the depth of indentations increase under larger Δp, that is under larger collapse velocity and also with the softer metal.
- For all the materials tested, the depth/diameter rate of the indentations is between 0.85 and 1.5 percent; those values are approximately the same as those reported in the literature (Belahadji et al., 1991).

Consequently, these observations lead us to think that in the final stage of the collapse, the erosion process, is dominated by the mechanisms which result from the implosion and rebounds of spherical bubbles. Those bubbles are isolated in space, but they are perhaps subject to reciprocal interactions. Now the problem is to know the way in which these events appear from the cavitating vortex flow. A possible scenario is that the large amount of bubbles are formed in the final torus described previously, which itself seems to result from instabilities of the vapour core free surface. But at the present time it is not possible to say if unstabilities are fundamental or if they result from the strong excitation of the mechanical system by the shock of the projectile on the piston head. However, the experimental work has allowed us to evaluate the moments when the critical events of the erosion take place.

7 Conclusion

A new device for the study of cavitation erosion due to the axial collapse of a cavitating vortex was presented. The three main parameters of the flow in this device can be controlled. The apparatus appears to be efficient as each shot produces a significant number of erosion indentations on metallic targets. Collapse velocities between 70 and 700 m/s are realized. Direct pressure measurements by a small transducer allowed us to identify the critical erosive instants. The visualization tests show the final stage of the axial vortex collapse at those critical instants when a two-phase torus is formed against the metal target or pressure transducer. A good correlation between the axial vortex evolution and the first appearance of the impulsive pressure has been observed. The pressure peaks and the presence of a number of pits over the impacted area seem to indicate that the targets are subject to a large number of local impulsive pressures. They probably result from the collapse and rebound of the spherical bubbles which are formed by the disintegration of the two-phase torus. Some reciprocal interactions are also possible. Finally, the duration of the high pressure final stage is of the order of 50 microseconds after the axial collapse, and the future work must be concentrated on this time interval.

Acknowledgments

The present project was supported by the "Direction des Recherches, Etudes et Techniques" (contracts N° 89-072 and 91-115), Ministry of Defence, France.

References

Avellan, F., and Farhat, M., 1989 "Shock Pressure Generated by Cavitation Vortex Collapse," ASME Fluids Engineering Conference, San Francisco, Proceedings pp. 119–125.

Belahadji, B., Franc, J. P., and Michel, J. M., 1991, "A Statistical Analysis of Cavitation Erosion Pits," ASME JOURNAL OF FLUIDS ENGINEERING, Vol. 113, No. 4, pp. 700–706.

Belahadji, B., Franc, J. P., and Michel, J. M., 1995 "Cavitation in the Rotational Structures of a Turbulent Wake," *Journal of Fluid Mechanics,* Vol. 287, pp. 383–403.

Benjamin, T., Ellis, A., 1966 "The Collapse of Cavitation Bubbles and the Pressure Thereby Produced Against Solid Boundaries," *Phil. Transactions,* Vol. A 260, pp. 221–240.

Blake, J., Taib, B., and Doherty, G., 1987 "Transient Cavities Near Boundaries. Part 2. Free Surface," *Journal of Fluid Mechanics,* Vol. 181, pp. 197–212.

Dominguez-Cortazar, M. A., Franc, J. P., and Michel, J. M., 1992 "Cavitating Vortex: Collapse Visualisation and Induced Damage," Third International I.Mech.E.Conference, Cambridge (U.K.), *Proceedings,* pp. 43–48.

Dominguez-Cortazar, M. A., 1994, "Le Cavermod, Modèle Physique de l'Erosion de Cavitation: Qualification Expérimentale et Numérique," Thesis, Joseph Fourier University, Grenoble (France), pp. 73–84.

Dominguez-Cortazar, M. A., and Canot, E., 1995 "Axial Collapse of a Cavitating Vortex: Numerical Simulation by an Integral Method," *International Symposium on Cavitation,* Deauville (France), *Proceedings,* pp. 459–464.

Fujikawa, S., and Akamatsu, T., 1980, "Effects of the Non-equilibrium Condensation of Vapour on the Pressure Wave Produced by the Collapse of a Bubble in a Liquid," *Journal of Fluid Mechanics,* Vol. 97, Part 3, 1980, pp. 481–512.

Hickling, R., and Plesset, M., 1963, "The Collapse of a Spherical Cavity in a Compressible Liquid," Div. of Eng. and Appl. Sciences, Report n° 85-24, California Institute of Technology.

Karimi, A., 1988, "Modèle Mathématique pour la Prediction de la Vitesse d'Erosion," *La Houille Blanche,* N° 7/8, pp. 571–576.

Lauterborn, W., and Bolle, H., 1975, "Experimental Investigation of Cavitation Bubble Collapse in the Neighbourhood of a Solid Boundary," *Journal of Fluid Mechanics,* Vol. 72, n° 2, 1975, pp. 391–399.

Le, Q., Franc, J. P., and Michel, J. M., 1993, "Partial cavities: Pressure Pulse Distribution Around Cavity Closure," ASME JOURNAL OF FLUIDS ENGINEERING, Vol. 115, No. 2, pp. 249–254.

Lecoffre, Y., 1978, "Cavitation Erosion by Shot Vortex," ASME, *Cavitation and Polyphase Flow Forum.*

Lecoffre, Y., Marcoz, J., and Valibouse, B., 1981, "Generator of Cavitation Vortex," ASME, Fluids Engineering Conference, Boulder.

Plesset, M., and Chapman, R., 1971, "Collapse of an Initially Spherical Vapour Cavity in the Neighbourhood of a Solid Boundary," *Journal of Fluid Mechanics,* Vol. 47, Part 2, 1971, pp. 283–290.

Rosenthal, D. K., 1962, "The Shape and Stability of a Bubble at the Axis of a Rotating Liquid," *Journal of Fluid Mechanics,* Vol. 12, 1962, pp. 358–386.

Selim, S., and Hutton, S., 1983, "Classification of Cavity Mechanics and Erosion," Second International I.Mech.E. Conference, *Proceedings,* pp. 41–49.

Soyama, H., Kato, H., and Oba, R., 1992, "Cavitation Observations of Severely Erosive Vortex Cavitation Arising in a Centrifugal Pump," *Third International I.Mech. E Conference,* Cambridge, Proceedings pp. 103–110.

Tomita, Y., and Shima, A., 1986, "Mechanisms of Impulsive Pressure Generation and Damage Pit Formation by Bubble Collapse," *Journal of Fluid Mechanics,* Vol. 169, pp. 535–564.

Vogel, O., Lauterborn, W., and Tiram, R., 1989, "Optical and Acoustic Investigations of the Dynamics of Laser-Produced Cavitation Bubbles Near a Solid Boundary," *Journal of Fluid Mechanics,* Vol. 206, 1989, pp. 299–338.